

normalized to the integrated reflecting power for $B_0/B_1 = 0$ for some values of φ . For large values of B_0/B_1 , R^θ tends to $(\pi/2)B_1(\cos \varphi + \sin \varphi)$ in each case, as was pointed out before.

2. Asymmetrical Laue case

For this case explicit results for the reflecting power are only known for $\varphi = 0$, $\varphi = 90^\circ$ and $B_0/B_1 \gg 1$. In

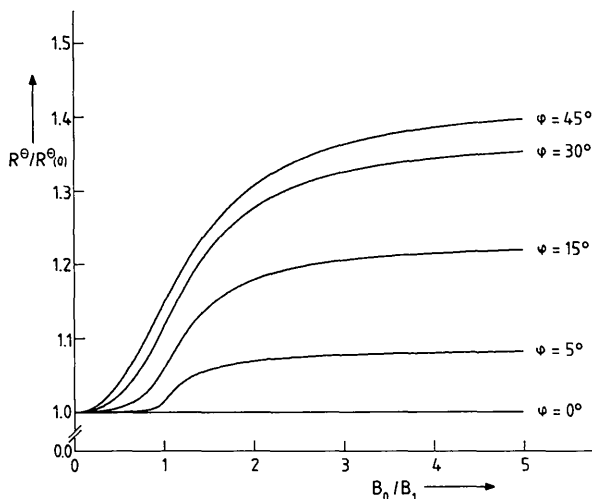


Fig. 2. Integrated reflecting power as a function of B_0/B_1 normalized to the value for $B_0/B_1 = 0$ for $\varphi = 0, 5, 15, 30$, and 45° .

Acta Cryst. (1983). **A39**, 682–685

Experiments on Dynamical Magnetic Neutron Diffraction by DyFeO_3

BY H. H. SCHMIDT, K. KÖNIG AND H. DANIEL

Physik-Department der Technischen Universität München, D-8046 Garching, Federal Republic of Germany

(Received 16 August 1982; accepted 8 March 1983)

Abstract

The integrated reflecting powers of two nuclear and one magnetic reflexions of a DyFeO_3 crystal have been measured. The results indicate that dynamical magnetic diffraction occurs. In addition, the integrated reflecting power of the magnetic reflexion was measured as a function of the magnetic field applied to the crystal. The results are discussed.

1. Introduction

Dynamical diffraction of thermal neutrons has been demonstrated by various experiments (Knowles, 1956; Sippel, Kleinstück & Schulze, 1965; Shull, 1968).

the first two cases one obtains the familiar result. In the third case, as for $b = 1$, the reflection curve splits into two Lorentzian peaks and the integration can be done easily. The result for R^θ is then the same as for $b = 1$ apart from a factor \sqrt{b} due to the broadening of the peaks.

The author wishes to thank Professor H. Daniel for his encouragement throughout this work.

References

- BELYAKOV, V. A. & BOKUN, R. CH. (1975). *Sov. Phys. Solid State*, **17**, 1142–1145.
 BELYAKOV, V. A. & BOKUN, R. CH. (1976). *Sov. Phys. Solid State*, **18**, 1399–1402.
 EKSTEIN, H. (1949). *Phys. Rev.* **76**, 1328–1331.
 GUIGAY, J. P. & SCHLENKER, M. (1978). *Acta Cryst.* **A34**, S229.
 GUSAKOV, A. G. & RUBAN, V. A. (1975). *Sov. Phys. Solid State*, **17**, 1972–1973.
 MENDIRATTA, S. K. & BLUME, M. (1976). *Phys. Rev.* **14**, 144–154.
 SCHMIDT, H. H., DEIMEL, P. & DANIEL, H. (1975). *J. Appl. Cryst.* **8**, 128–131.
 SCHMIDT, H. H. & DEIMEL, P. (1975). *J. Phys. C*, **8**, 199–1996.
 SCHMIDT, H. H. & DEIMEL, P. (1976). *Phys. Status Solidi B*, **73**, 87–93.
 SIVARDIÈRE, J. (1975). *Acta Cryst.* **A31**, 340–344.
 STASSIS, C. & OBERTEUFFER, J. A. (1974). *Phys. Rev. B*, **10**, 5192–5202.
 ZACHARIASEN, W. H. (1945). *Theory of X-ray Diffraction in Crystals*. New York: Wiley.

However, in all these experiments diffraction is only due to nuclear scattering. Dynamical magnetic diffraction was never observed. The theory of dynamical magnetic neutron diffraction was recently treated by Schmidt & Deimel (1976), Belyakov & Bokun (1976), Guigay & Schlenker (1978), and Schmidt (1983). The diffraction process depends on the angle φ between \mathbf{B}_A , the average magnetic field in the crystal, and \mathbf{B}_H , the Fourier transform of the magnetic field with respect to the scattering vector, and on the ratio B_A/B_H with $B_A = |\mathbf{B}_A|$ and $B_H = |\mathbf{B}_H|$. The aim of the experiments described here was twofold: firstly to establish dynamical magnetic neutron diffraction experimentally, and secondly to test the theoretical statements of Schmidt (1983).

2. The crystal

A single crystal of DyFeO_3 was used. DyFeO_3 is an antiferromagnet, which has reflexions of pure nuclear origin (e.g. $2\bar{2}0$) and $\bar{1}30$) and reflexions of pure magnetic origin (e.g. 031). A slight canting of the magnetic moments gives rise to a small 'parasitic' spontaneous magnetic moment along the c axis (Sherwood, Remeika & Williams, 1959) of about 0.07 Bohr magnetons ($6.5 \times 10^{-25} \text{ JT}^{-1}$) (Godoretsky, Sharon & Shtrikman, 1968) yielding an average magnetic field of about 14 mT. Fields up to 1.8 T do not influence the magnitude and direction of the spontaneous magnetic moment (Sherwood, Remeika & Williams, 1959). Thus, \mathbf{B}_H is a constant vector independent of an external magnetic field and \mathbf{B}_A is essentially defined by the external field. Therefore it is possible to choose the value of B_A/B_H as well as the angle φ by applying an external magnetic field of appropriate magnitude and direction to the crystal.

The crystal used here has the dimensions $17.0 \times 4.4 \times 0.47$ mm. It is stated by the supplier (Crystal-Tec, Grenoble) that the density of dislocations is less than 1000 cm^{-2} . X-ray diffraction measurements showed a mosaic spread of about $12''$. X-ray topographs taken with Mo $K\alpha$ radiation showed anomalous transmission to occur.

3. Experimental arrangement

The measurements were performed at the reactor FRM in Garching. Two different set-ups were used, shown in Fig. 1. A Si monochromator was used in both. The Bragg angle was 19° and the neutron wavelength was 1.26 \AA . The neutron flux incident at the Si crystal was about $3 \times 10^{11} \text{ m}^{-2} \text{ s}^{-1}$. In set-up 2 the crystal was situated within the pole gap of a magnet, which allowed the application of a magnetic field between zero and 0.8 T corresponding to a variation of B_A/B_H from 0 to 1.58. φ was 76.7° . The detectors shown in Fig. 1 were scintillators sensitive to slow neutrons. They were

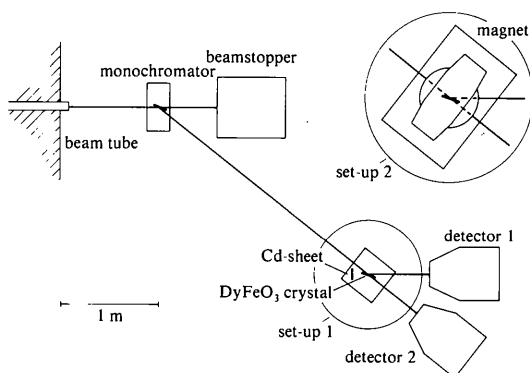


Fig. 1. Experimental set-ups.

shielded with 1 mm Cd and approximately 20 cm water. In the case of the measurements with set-up 1, a 1 mm thick Cd sheet was placed behind the DyFeO_3 crystal.

4. Experiments and results

(a) Measurements with set-up 1

The reflexion curves of the two nuclear reflexions $2\bar{2}0$ and $\bar{1}30$, and of the magnetic reflexion 031 of DyFeO_3 were measured several times. Furthermore, calibration runs were performed with the $2\bar{2}0$ reflexion of a perfect Si crystal of the same shape as the DyFeO_3 crystal. From the reflexion curves the integrated reflected intensities were obtained and from these, using the results of the calibration runs, the absolute values of the integrated reflecting power were calculated. These values are shown in Table 1. For each reflexion the weighted mean of the values of the integrated reflecting power obtained from the various measurements is also given.

(b) Measurements with set-up 2

Reflexion curves of the magnetic 031 reflexion with different values of the magnetic field on the crystal were measured and from them the unnormalized values of the integrated reflected intensity were obtained. The results are shown in Table 2.

Table 1. Experimental values of the integrated reflecting power of the DyFeO_3 reflexions

Reflexion	Run no.	$R_{\text{exp}}^{\theta} \times 10^5$
$2\bar{2}0$	1	3.29 ± 0.05
$2\bar{2}0$	2	3.26 ± 0.03
$2\bar{2}0$	Mean	3.27 ± 0.03
$\bar{1}30$	1	1.25 ± 0.14
$\bar{1}30$	2	1.28 ± 0.32
$\bar{1}30$	3	1.22 ± 0.46
$\bar{1}30$	Mean	1.25 ± 0.12
031	1	2.01 ± 0.26
031	2	2.16 ± 0.12
031	Mean	2.13 ± 0.11

Table 2. Experimental values (column 4) of the integrated intensity of the 031 reflexion of DyFeO_3 for different values of the magnetic field (column 2); in column 3 B_A/B_H is given

Run no.	B (T)	B_A/B_H	$I_{\text{exp}} \times 10^5$
1	0.00	0.00	2.17 ± 0.18
2	0.04	0.09	2.05 ± 0.17
3	0.08	0.18	2.01 ± 0.27
4	0.52	1.14	2.56 ± 0.22
5	0.72	1.58	2.16 ± 0.19
6	0.72	1.58	2.40 ± 0.17

5. Discussion

(a) Measurements with set-up 1

In column 5 of Table 3 the values of $y_{\text{exp}} = R_{\text{exp}}/R_{\text{kin}}$ are given, where y_{exp} is the experimental extinction factor, R_{exp} is the experimental integrated reflecting power, and R_{kin} is the calculated kinematical reflecting power. The extinction factor can be written as $y = y_p y_s$, where y_p and y_s are due to primary and secondary extinction, respectively. To obtain an estimation for y_p two simple mosaic block models were used, one with blocks of a spherical shape (Becker & Coppens, 1974), and one with blocks with the shape of a square-sectioned parallelepiped (Olekhovich & Olekhovich, 1978). The secondary extinction factor y_s was calculated according to Bonnet, Delapalme, Becker & Fues (1976), always assuming a Lorentzian shape for the reflexion curve of the single blocks, as well as for the angular distribution function of the blocks. The mosaic block thickness t_M and the width of the angular distribution function η were obtained by a least-squares fit to the values of y_{exp} for both the sphere and the parallelepiped models. For the sphere model, the value of the normalized χ^2 was 36, whereas with the parallelepiped model a value of $\chi^2 = 2.7$ was obtained. Hence the latter model was finally used. For t_M and η the following values were obtained:

$$t_M = (70 \pm 3) \mu\text{m}$$

$$\eta = (3.2 \pm 1.3) \times 10^{-5}$$

In Table 3 the values of y_p , y_s and y are summarized together with the values y_{exp} for the three reflexions used. They indicate that primary extinction is predominant for the crystal and the reflexions used. Because this is also true for the magnetic reflexion, we state that dynamical magnetic diffraction was observed in this experiment.

(b) Measurements with set-up 2

Fig. 2 shows the theoretical values of the integrated reflecting power of the magnetic reflexion as a function of B_A/B_H normalized to the value for $B_A/B_H = 0$ for $\varphi = 76.7^\circ$ (Schmidt, 1983). These values are the same for runs 5 and 6 and differ by much less than the

Table 3. Fitted values for the primary (column 2), the secondary (column 3) and the total extinction factor (column 4); in column 5 the measured values for the total extinction factor are given

Reflexion	y_p	y_s	y	y_{exp}
220	0.132 ± 0.008	0.72 ± 0.07	0.095 ± 0.006	0.0951 ± 0.0007
130	0.309 ± 0.024	0.91 ± 0.03	0.270 ± 0.016	0.31 ± 0.03
031	0.39 ± 0.03	0.931 ± 0.024	0.360 ± 0.020	0.339 ± 0.018

statistical errors for runs 1 to 3. Therefore the weighted means of the experimental values of runs 1 to 3 and of runs 5 and 6 were formed. In column 3 of Table 4 these mean values and the value for measurement 4 are given. In column 4 the ratios of the values of column 3 to the corresponding theoretical values are listed. The last two lines of Table 4 show the weighted means of column 3 and column 4 as well as the corresponding χ^2 values. χ^2 amounts to 1.0 for column 4 and 2.0 for column 3. Hence the experimental values are in better agreement with the predictions of the dynamical theory (Schmidt, 1983) than with those of the kinematical theory. However, statistics are not sufficient to exclude the absence of dynamical effects.

The authors wish to thank P. Stoeckel, H. Angerer and H. Hagn for valuable technical assistance.

Table 4. Means of the experimental values for the integrated intensity (column 3) for the different theoretical expectation values (column 2) and ratios between the experimental and the theoretical values (column 4)

Runs	$R = R^0 \left(\frac{B_A}{B_H} \right) / R^0(0)$	$I_{\text{exp}} \times 10^5$	$\frac{I_{\text{exp}}}{R} \times 10^5$
Mean 1-3	1.00	2.09 ± 0.11	2.09 ± 0.11
4	1.09	2.56 ± 0.22	2.35 ± 0.20
Mean 5-6	1.13	2.29 ± 0.13	2.03 ± 0.11
Overall mean		2.22 ± 0.08	2.10 ± 0.07
χ^2		2.01	1.0

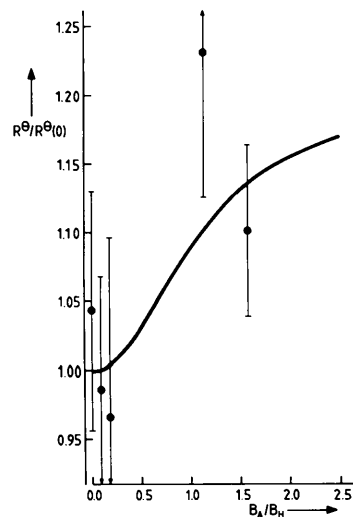


Fig. 2. Theoretical integrated reflecting power of the magnetic reflexion 031 of DyFeO₃ as a function of B_A/B_H and experimental values. The theoretical values are normalized to the value $B_A/B_H = 0$ and the experimental values are normalized so that the mean-square deviation from the theoretical values is a minimum.

References

- BECKER, P. J. & COPPENS, P. (1974). *Acta Cryst.* A30, 129–147.
 BELYAKOV, V. A. & BOKUN, R. CH. (1976). *Sov. Phys. Solid State*, 18, 1399–1402.
 BONNET, M., DELAPALME, A., BECKER, P. & FUESS, H. (1976). *Acta Cryst.* A32, 945–953.
 GORODETSKY, G., SHARON, B. & SHTRIKMAN, S. (1968). *J. Appl. Phys.* 39, 1371–1372.
 GUIGAY, J. P. & SCHLENKER, M. (1978). *Acta Cryst.* A34, S229.
 KNOWLES, J. W. (1956). *Acta Cryst.* 9, 61–69.
 OLEKHNovich, N. M. & OLEKHNovich, A. I. (1978). *Acta Cryst.* A34, 321–326.
 SCHMIDT, H. H. (1983). *Acta Cryst.* A39, 679–682.
 SCHMIDT, H. H. & DEIMEL, P. (1976). *Phys. Status Solidi B*, 73, 87–93.
 SHERWOOD, R. C., REMEIK, J. P. & WILLIAMS, H. J. (1959). *J. Appl. Phys.* 30, 217–225.
 SHULL, C. G. (1968). *Phys. Rev. Lett.* 21, 1585–1589.
 SIPPEL, D., KLEINSTÜCK, K. & SCHULZE, G. E. R. (1965). *Phys. Lett.* 14, 174–175.

Acta Cryst. (1983). A39, 685–692

From a Partial to the Complete Crystal Structure

BY CARMELO GIACOVAZZO

Istituto di Mineralogia e Petrografia, Università, Palazzo Ateneo, 70121 Bari, Italy

(Received 15 October 1982; accepted 28 March 1983)

Abstract

The joint probability distribution method is applied in order to estimate phases when part of the crystal structure is correctly positioned. The mathematical approach is briefly described and the conclusive formulas are compared with those given by previous authors.

Symbols and abbreviations

Throughout the paper a number of symbols will find frequent application. For the sake of simplicity they are here listed together.

$\mathbf{h} \equiv (h, k, l)$: vectorial index of a reflection. We will also use \mathbf{k} and $\mathbf{h} + \mathbf{k}$.

$f(\mathbf{h})$: atomic scattering factor. The thermal factor is included: anomalous dispersion is not considered.

$F_{\mathbf{h}}$: structure factor with vectorial index \mathbf{h} .

N : number of atoms in the unit cell.

p : number of atoms (symmetry equivalents included) whose positions are *a priori* known.

q : number of atoms (symmetry equivalents included) whose positions are unknown: $q = N - p$.

$F_{\mathbf{h}}, E_{\mathbf{h}}$: structure factor and normalized structure factor with vectorial index \mathbf{h} .

$\varphi_{\mathbf{h}}, \varphi_{\mathbf{k}}, \varphi_{\mathbf{h} + \mathbf{k}}$: phase values of $E_{\mathbf{h}}, E_{\mathbf{k}}, E_{\mathbf{h} + \mathbf{k}}$.

$R_{\mathbf{h}}, R_{\mathbf{k}}, R_{\mathbf{h} + \mathbf{k}}$: moduli of $E_{\mathbf{h}}, E_{\mathbf{k}}, E_{\mathbf{h} + \mathbf{k}}$.

$\Phi = \varphi_{\mathbf{h}} + \varphi_{\mathbf{k}} - \varphi_{\mathbf{h} + \mathbf{k}}$.

$E_{p, \mathbf{h}}, E_{p, \mathbf{k}}, E_{p, \mathbf{h} + \mathbf{k}}$ = pseudo-normalized structure factors of the partial structure with p atoms in the unit cell.

$R_{p, \mathbf{h}}, R_{p, \mathbf{k}}, R_{p, \mathbf{h} + \mathbf{k}}$: moduli of $E_{p, \mathbf{h}}, E_{p, \mathbf{k}}, E_{p, \mathbf{h} + \mathbf{k}}$.

$\varphi_{p, \mathbf{h}}, \varphi_{p, \mathbf{k}}, \varphi_{p, \mathbf{h} + \mathbf{k}}$ = phase values of $E_{p, \mathbf{h}}, E_{p, \mathbf{k}}, E_{p, \mathbf{h} + \mathbf{k}}$.

$\Phi_p = \varphi_{p, \mathbf{h}} + \varphi_{p, \mathbf{k}} - \varphi_{p, \mathbf{h} + \mathbf{k}}$.

$E_{q, \mathbf{h}}, E_{q, \mathbf{k}}, E_{q, \mathbf{h} + \mathbf{k}}$ = pseudo-normalized structure factors of the unknown part of the structure.

$R_{q, \mathbf{h}}, R_{q, \mathbf{k}}, R_{q, \mathbf{h} + \mathbf{k}}$ = moduli of $E_{q, \mathbf{h}}, E_{q, \mathbf{k}}, E_{q, \mathbf{h} + \mathbf{k}}$.

$$\Sigma_q(\mathbf{h}) = \sum_{j=p+1}^N f_j^2(\mathbf{h}).$$

$t_j(\mathbf{h}) = f_j(\mathbf{h}) / [|F_{p, \mathbf{h}}|^2 + \Sigma_q(\mathbf{h})]^{1/2}$ for the j th atom.

$$b(\mathbf{h}) = \sum_{j=p+1}^N t_j^2(\mathbf{h}) = \Sigma_q(\mathbf{h}) / [|F_{p, \mathbf{h}}|^2 + \Sigma_q(\mathbf{h})].$$

$$c = \sum_{j=p+1}^N t_j(\mathbf{h}) t_j(\mathbf{k}) t_j(\mathbf{h} + \mathbf{k}).$$

Other locally used symbols are defined in the text.

1. Introduction

Main (1976) generalized Cochran's (1955) formula for the phase probability of a triple product in order to exploit some *a priori* knowledge about the structure. He considered four kinds of information: (a) randomly positioned atoms; (b) randomly positioned and randomly oriented atomic groups; (c) randomly positioned but correctly oriented atomic groups; (d) correctly positioned atoms.

A mathematical derivation of Main's formula was given by Heinerman (1977) (see also Heinerman, Krabbendam & Kroon, 1977). In its formulation the normalized structure factor $E_{\mathbf{h}}$ is defined by